A Comprehensive approach towards efficient removal of fluoride along with co-existing pollutants from real groundwater using electrocoagulation process

Daisy Das*[a,b], Barun Kumar Nandi*[a]

[a]*Department of Fuel, Minerals and Metallurgical Engineering, Indian Institute of Technology (Indian School of Mines), Dhanbad, Jharkhand-826004, India*

[b] *Current affiliation: Micro & Nano Systems Centre, Tyndall National Institute-University College Cork, Lee Maltings, Dyke Parade, T12 R5CP, Cork, Ireland*

*Corresponding author: E-mail: daisydas89@gmail.com; barun@iitism.ac.in; Phone: +91 3262235139; Fax: +91 3262296563,

Abstract

This study evaluated the effectiveness of Electrocoagulation (EC) in treating fluoride-contaminated groundwater from Gharbar village, Jharkhand, where fluoride concentrations range from 3.76 to 12.9 mg L^{-1} along with other co-existing ions. The order of abundance of anions was sulfate > fluoride > nitrate > potassium > phosphate > chlorine, and for cations, it was magnesium > calcium. Optimal EC conditions were achieved for five groundwater samples (S1 to S5), with fluoride removal efficiencies from 89.58% to 96.40%, attaining the safe threshold of 1 mg L^{-1}. The process utilizes an electric potential of 12 V, an electrode gap of 0.5 cm, and a treatment time of 3600 s, using aluminium electrodes in bipolar mode. An additional adsorption step with activated charcoal (1g $3L^{-1}$) for 1800 s enhanced the treated water quality, reducing hardness, alkalinity, and turbidity, achieving fluoride removal rates between 93.45% and 99.82%. To replace laboratory-scale filter paper methods for floc separation, commercial ceramic candle-based filters and carbon gravity filters were employed. Analysis of the sludge field emission scanning electron microscopy and energy-dispersive X-ray analysis confirmed the capture of fluoride and other ions in metal hydroxide flocs. Kinetic analysis indicated that fluoride ion removal followed the first-order kinetic model. The optimized electrocoagulation process demonstrated an electric energy consumption of 3.2 kWh m^{-3}, electrode consumption of 0.2684 g L^{-1}, and theoretical H_2 generation of 0.3581 L. The operating cost was estimated at 0.5030 US$ m^{-3} for electrocoagulation alone and 0.5185 US$ m^{-3} with adsorption and filtration, highlighting the feasibility and cost-effectiveness of this hybrid approach for fluoride removal from groundwater.

Keywords: Electrocoagulation, Groundwater contamination, Fluoride removal, Activated charcoal, Aluminium electrodes

1. Introduction:

Geogenic pollution of groundwater has been a significant challenge in environmental science in recent decades [1]. Groundwater contamination with fluoride and its related dental and skeletal fluorosis endemic influences over 200 million global populations in 35 nations [1-3]. Fluorosis is a serious health concern in India, where excessive fluoride consumption in drinking water puts more than 67 million people in 20 states in danger [2,4]. Prolonged consumption of drinking water containing fluoride concentration above 1.0 mg/L leads to several health issues such as osteoporosis, weak bones, cancer, infertility in women, Alzheimer's syndrome and thyroid disorder [5]. However, fluoride intake below 1 mg/L helps prevent skeletal issues and dental caries [1]. Besides fluoride occurring in the environment due to fluoride-containing minerals, such as fluorite (CaF_2), biotite [$K(Mg, Fe)_3AlSi_3O_{10}F_2$], topaz [$Al_2SiO_4(FOH)_2$], fluor-apatite [$Ca_5(PO_4)_3F$], etc., in the earth's crust, many industrial activities also contribute to fluoride generation; these include semiconductor, electroplating, etc. [2-3]. The physicochemical properties of groundwater depend upon the hydrology of groundwater in hydrogeological conditions based on factors such as underlying geology, rock type, rock-water interaction, temperature, solubility, pH and accessibility of fluorine, etc. [5-7]. The prevalence of fluoride in groundwater of Gharbar village, Dhanbad, India in concentrations as high as 18.5 mg L^{-1} along with coexistence NO_3^- of have been reported previously [5, 8]. However, the presence of a high amount of co-existing ions in the groundwater along with high fluoride concentration has not been reported in any studies. Furthermore, the majority of studies have predominantly concentrated on conducting detailed geochemical analyses in the region to delineate the processes responsible for the release of fluoride. Patolia and Sinha 2007 [8], report the presence of fluoride in the 0.3 to 14.9 mg L^{-1} in the groundwater of Gharbar village and demonstrate its release is due to the geochemical composition

of rock and dominated mainly by hornblende and biotite as fluoride-bearing minerals. Thapa et al., 2019 [5], also report the occurrence of fluoride in the range of 0.01 to 18.55 mg L^{-1} in Gharbar village, Jharkhand, along with the co-occurrence of high concentration of nitrate and bicarbonate ions. Generally, high F^- groundwater has an alkaline pH with Mg/Ca hardness and a high concentration of Al, nitrate, etc. [8]. The toxic effect of co-existing pollutants in drinking water, mainly fluoride with the concurrent occurrence of nitrate, arsenic, and other cations like Ca and Mg in excess can be a source of various diseases like Alzheimer's disease as well as its neurotoxicity among the inhabitant [9-12]. Because the area is semi-arid, the only viable solution for drinking water at the site is groundwater. Thus, groundwater defluoridation is extremely important regarding the compelling and feasible utilization of environmental management.

Several techniques for defluoridation from groundwater have been reported, which include membrane separation, coagulation, ion-exchange, adsorption, oxidation/regeneration, and electrocoagulation [13-22]. Among all these methods, oxidation/regeneration and coagulation/precipitation have been widely used for fluoride removal. However, such methods have many drawbacks, like more significant production of sludge, sensitivity to pH, and less removal efficiency [23]. Therefore, development of a compact, easy-to-operate, and low-cost process for treatment of such contaminated groundwater seems to be an essential contribution to overcoming these limitations. The electrocoagulation process is a possible simple and cost-effective alternative to conventional physicochemical methods [24-26]. Adsorption is another attractive way of removing pollutants from wastewater due to the potential of using low-cost and environmentally friendly [16]. Activated carbon is the most used adsorbent in removing organic compounds from wastewater due to its high surface area and well-developed pore structure [7]. However, several low-cost adsorbents such as biochar, peanut shells, coal fly ash, rice husk, and

bagasse fly ash are alternatives for water treatment [27-31]. While electrocoagulation and adsorption processes hold significant promise for wastewater treatment, each comes with its own potential limitations during operation. The primary challenge associated with the electrocoagulation process often lies in its energy consumption, particularly when addressing highly concentrated effluents. As reported in much literature, electrocoagulation is an efficient technique for the removal of various pollutants in higher concentration ranges by altering its significant operating conditions like current density, number of electrodes and salt dose [32]. However, operating the process in a higher range of current density, increasing the number of electrodes and higher salt dose, increases the system's operating cost, and the quality of the treated water may be compromised due to retaining some secondary pollutants like Al, Na, Cl, etc. This may happen because of excess formation of metal hydroxide due to higher dissolution of metal electrodes at more current density. The inclusion of a subsequent adsorption step in the electrocoagulation process can be the solution as it may add to the removal of other secondary pollutants which are generated mostly due to excessive dissolution of electrode material. Also, particulate matter will delay the adsorbent saturation and mitigate the inhibitory effects. Moreover, most of the EC treatments reported have used filter paper for filtering the flocs generated, which is only viable in the lab-scale process. So, replacing the filtration medium with any commercially available ceramic filtration unit may be helpful to upscale the application of the EC process. The advantage of a subsequent adsorption and filtration step in the electrocoagulation process offers a practical solution to mitigate secondary pollution arising from excess metal dissolution at high current densities, while also enhancing the overall water quality and enabling scalable application through the use of commercially available filtration units.

This study aims to assess the potential effectiveness of the EC process in efficiently removing fluoride from natural groundwater. A comprehensive exploration of the EC method will be presented, covering experimental results and examining the impact of critical operating parameters such as applied electric potential (V), electrode connection mode, electrode material, and electrode distance (ID). Considering the presence of various co-existing pollutant ions in groundwater alongside fluoride, optimizing EC operating parameters to eliminate all these ions up to permissible limits is crucial, ensuring the water meets drinkable quality standards. To treat such highly contaminated groundwater, operating parameters of EC like applied potential may be on the higher side, leading to more anodic corrosion and retaining secondary pollutants in the treated water. An adsorption study will be conducted after 3600 s of EC, employing varying dosages of analytical-grade activated charcoal to address this challenge.

Additionally, the investigation will explore the substitution of laboratory-based filter paper with commercially available ceramic filtration units and gravity carbon filters as filtration media to achieve potable water quality. The treated water will be analyzed for predominant contaminants such as TDS, alkalinity, salinity, Mg^{2+}, Al^{3+} ions, as well as other coexisting anions and cations after each treatment process, including electrocoagulation (EC), adsorption, and filtration.

To evaluate the economic feasibility of the EC process, assessments will be made for electric energy consumption (EEC), electrode consumption, theoretical hydrogen gas yield, and operating costs. The findings from this study are anticipated to furnish essential information and data for the development of an affordable household purification unit.

2. Materials and methods:

2.1 Experimental:

Batch EC experiment was conducted for 3 L of sample water in a glass beaker at room temperature. Aluminum (Al) and Iron (Fe) electrodes, measuring 10 cm in length, 5.8 cm in width, and 0.1 cm in thickness, with an effective area of 116 cm^2, were used. Different electrode connection mode like monopolar, bipolar, series monopolar, and combination of electrode material was investigated as per our previously reported work [25]. The schematic of the experimental setup is represented in Fig.1. To apply electric potential to the system, a DC power source was used from APLAB, India (Model: L6410S, 0-10 and 0-30V). A magnetic stirrer from TARSON, India (Model: SPINIT Digital MC-02) was used for homogeneous stirring of the solution during EC. The electrodes were cleaned after each experiment by scrubbing and rinsing with hydrochloric acid, followed by acetone and water. The polarity of the electrodes was changed after each investigation for proper utilization. During EC experiments, a sample of around 5-7 ml at 600 s intervals was collected and subsequently filtered using Whatman 1 filter paper (0.42µm) for the essential analyses. The fluoride concentration was determined using a fluoride ion-selective electrode from EUTECH, India. Before measurement, the electrode underwent essential calibration using a fluoride standard solution. Water quality parameters, including turbidity, total dissolved solids (TDS), salinity, conductivity, and pH, were assessed using a turbidity meter (Model: TN-100) from Thermo Scientific) and a multiparameter kit (Model: PC2700) from Eutech. The concentrations of iron (Fe) and aluminium (Al) ions were determined through flame method in an atomic absorption spectroscopy (AAS) (Model: iCE 3000 Series) from Thermo Scientific).

A photometer with automatic wavelength selection (Palintest Alkaphot PM188; Model: 7100, Make: UK) that operates based on the colorimetric method using tablet reagent specific to the target analyte was used to analyze the concentration of phosphate, nitrate, sulfate, alkalinity,

calcium, chlorine, magnesium, potassium, and hardness in the sample. For checking the hardness of water Palintest Hardicol No.1 and No.2 tablets that could detect hardness in the range of 0-500 mg/L $CaCO_3$ were used in 10 ml of sample. The pH required in the test is closely controlled by the buffer mixture in the tablet formulation as a high iron level in the sample will cause low hardness. However, highly acidic or basic samples should be adjusted in the range of pH 4 to 10 to avoid errors in the test. For analysis of sulfate in the sample Palitest sulfate Turb tablets were used which is suitable for detecting sulfate in the range of 0-200 mg L^{-1}. Similarly, for analysis of phosphate (Palintest phosphate tablet No 1 and No 2 LR Tablets; 0-4 mg L^{-1} PO_4; 0-1.3mg L^{-1} P), nitrate (Palintest Nitratest powder, tablet, and Nitricol tablets; 0-20 mg L^{-1}), calcium (Palintest Calcicole No1 and No2 tablets), chlorine (Palintest DPD-XF and DPD Oxystop tablets, 0-10 mg L^{-1}) and potassium (Palintest potassium K tablets; 0-12 mg L^{-1}) were used. The samples higher in concentration than the range of the reagent were analyzed by subsequent dilution and then multiplying the result by the dilution factor. The elemental composition of the sludge generated by EC was analyzed using field emission scanning electron microscopy with energy-dispersive X-ray analysis (FESEM-EDX) (Supra 55 MonoCL4 instrument from Carl Zeiss). For the adsorption study, activated charcoal of analytical grade from RANKEM India (Density: 2 g cm^{-3} (20 °C)) with a surface area of 883.9 m^2 g^{-1}, pore diameter of 2 nm and pore volume of 0.26 cm^3 g^{-1} was used. For a survey of filtration medium, a commercially available gravity filter with ceramic candles (Pore diameter of 0.15 to 0.5 microns) and a gravity water filtration unit based on ultrafiltration technology (nano-silver carbon-based disinfection) were used. Experiments were performed with various ranges of parameters to investigate different process parameters, as shown in Table S1. The reaction time for the electrocoagulation process was determined through preliminary experiments using a synthetic fluoride solution with an initial concentration of 20 mg

L^{-1}. At a constant applied electric potential of 12 V, samples were collected and analyzed at 600 s time intervals to evaluate fluoride removal efficiency. All the experiments were performed for 3600 s, and the adsorption test was conducted for 1800 s and, for accuracy, repeated thrice with a variation of ± 0.5%. Fluoride concentration after each 600 s was recorded, and the final concentration after 3600 s was reported. The equation used to estimate the removal efficiency of fluoride ions is as follows:

$$\text{Fluoride Removal (\%)} = \frac{C_0 - C_t}{C_0} \times 100 \qquad (1)$$

Here, C_o and C_t represent the fluoride ion concentration at the initial and after 3600 s of EC in mg/L respectively.

Pollutant removal during EC process can be illustrated by kinetic models of the first order as [23]

$$-ln\frac{C_o}{C} = kt \qquad (2)$$

Where C_0 and C is the initial concentration of fluoride ion and fluoride concentration at any EC time t respectively. First order rate constant k (s^{-1}) can be estimated from $ln(C_0/C)$ versus t plot, where the slope of the resulting straight line corresponds to the rate constant (k).

2.2 Estimation of theoretical hydrogen (H_2) gas yield, electric energy consumption and operating cost:

EC process generates H_2 gas as a primary by-product, known for its eco-friendly nature and considerable energy potential. The ability to harvest H_2 gas is a significant advantage of EC technology. For instance, research has indicated that approximately 5.8 to 13% of the electrical energy needed to operate an EC cell can be reclaimed by recycling the produced H_2 gas [20].

Theoretical hydrogen (H_2) gas produced at various current densities during EC was calculated using the following formula reported [36].

$$q_{H_2} = \frac{CD \times E_A \times t \times H_2}{F} \quad (3)$$

Where q_{H_2} , CD, E_A , t, H_2, F is the amount of H_2 gas emitted (mole), current density (A m^{-2}), the effective area of the electrode (m^2), reaction time (s), number of hydrogen molecules (0.5), and Faraday constant (96500) respectively. The amount of H_2 gas produced is expressed in a volumetric unit (L) as per the equation reported in the literature [20]. To estimate the energy yield from H_2 gas, the formula is given by [37]:

$$E_{H_2} = m(0.244 \frac{MJ}{mole}) \quad (4)$$

Here E_{H_2}, m are energy yield (MJ), and amount of H_2 gas (mole), respectively. It is crucial to emphasize that every 3.6 MJ can produce 1.0 kWh [20].

The calculation for the operating cost (OC) in US$ m^{-3} for treating 3L of fluoride-contaminated water by EC process for3600 sutes follows the formula [38]:

$$OC\ (US\$\ m^{-3}) = [p.C_{energy} + q.C_{electrode}] \quad (5)$$

Where p (0.083 US$ kW^{-1} h^{-1}) is the cost of electricity per unit and q (2.046 US$ kg^{-1} Al^{-1}) is the cost of Al per kg, respectively. These values are considered based on the Indian market price in 2018 [38].

$$C_{energy} = \frac{Cell\ voltage(V) \times current(A) \times time(s)}{sample\ volume(m^3)} \quad (6)$$

$$C_{electrode} = \frac{Applied\ current\ (A) \times reaction\ time\ (s) \times m_w}{z \times F \times sample\ volume\ (m^3)} \quad (7)$$

Here m_w, z and F denote the molecular mass of Al (26.981 g mol^{-1}), chemical equivalence (z=3), Faraday's constant (96487 C mol^{-1}) respectively.

The overall cost of the integrated process which is EC, adsorption and filtration are as follows:

$$Total\ cost\ (TC)\ (US\$/m^3) = [OC + AC + FC] \quad (8)$$

Where OC is the operating cost of 3600 s of the EC process estimated as per Eqn. 5, AC is the cost of the adsorbent per gram to treat per litre of sample in US$ m^{-3}. FC is the total cost of filtration, which is considered the cost of the ceramic filter and its reusability or lifespan to treat the maximum volume of water.

In this study to treat 3L of water, 1g of commercially available activated charcoal was used, costing 0.009 US$ considering the price of commercially available activated charcoal is 9-10 US$ per kg. [35].

Moreover, a pair of locally available Indian-made ceramic filter candles cost around 1-2 US$ and can be used for 6-8 months to filter around 14 litres of water per day with a flow rate of 1-2 L hr^{-1} per candle [39]. Considering this the FC for this study is around 0.0065 US$.

Electric energy consumption (EEC) per unit volume (KWh m^{-3}) can be calculated as follows [24]:

$$\mathrm{EEC} = \frac{\text{cell volatge (v)} \times \text{Applied current (A)} \times \text{Time of EC (hr)}}{\text{sample volume } (m^3)} \qquad (9)$$

Here, the volume of the sample (ν = 0.003 m^3).

The determination of overall anodic dissolution (g L^{-1}) during EC was calculated using Faraday's law as follows [24]:

$$M = \frac{Applied\ Current\ (A) \times EC\ time(s) \times molecular\ mass\ of\ anode\left(\frac{g}{mol}\right)}{Chemical\ equivalence(Z) \times Faradays\ constant\ \left(96485\frac{C}{mol}\right)} \qquad (10)$$

3. Sampling and characterization of groundwater:

The groundwater samples were collected from Gharbar village (23°24′57″N 86°31′27″E), situated at 9 km from Baliapur and 23 km from Dhanbad, India, which is a prominent fluoride-affected zone in eastern India. Groundwater samples were collected from five different tube wells used for drinking and other household usage purposes located at about 500 m distance. Approximately 60

L of water each from five different sources was collected and tested for various water quality parameters within 1 hr. The fluoride concentration range measured was 3.76-12.9 mg L^{-1}, consistent with earlier investigations' findings [5,8, 33-34]. The groundwater samples were characterized in detail, and the key parameters are listed in Table 1. The analysis of the groundwater samples shows that fluoride exceeds the permissible limit in drinking water, i.e.,>1 mg L^{-1}. The order of abundance of anions and cations are: $SO_4^{-2} > F^- > NO^-_3 > K^- > PO_4^- > Cl^-$ and $Mg^{2+} > Ca^{2+}$respectively. The turbidity, conductivity, salinity, TDS, pH, alkalinity and hardness for all the samples (S1-S5) were found in the range of 1.07- 10.31 NTU, 731-2228 µS cm^{-1}, 231-1198 mg L^{-1}, 532-1610 mg L^{-1}, 7.45-7.94, 195-651 mg L^{-1} and 45-460 mg L^{-1} respectively.

4. Results and Discussions

4.1 Selection of cathode and anode material combination:

Fig.2 shows the combination of cathode and anode material for the efficient removal of fluoride for all the samples in this study. From Fig. 2, it is noticed that Al as anode material shows better removal efficiency for fluoride for all the samples. For S1, the removal efficiency of fluoride with a combination of cathode and anode material as Al/Al, Fe/Fe, Al/Fe, and Fe/Al are 89.6%, 41.7%, 59.9%, and 67.9%, respectively. Similarly, for S2, the removal efficiencies at Al/Al, Fe/Fe, Al/Fe, and Fe/Al combination are 91.9%, 50.8%, 77.7%, and 80.7%, respectively. Similar trends of results are found for S3, S4 and S5. Removal efficiencies for S3, S4, S5 at Al/Al, Fe/Fe, Al/Fe, and Fe/Al combination are 96.4%, 36.6%, 44.4%, 54.4%; 92.6%, 38.8%, 41%, 44.2% and 87.5%, 40.6%, 47.8%, 51.4% respectively. The removal increased by 3-12% when Al was used as anode material and Fe as cathode material for all the samples. Removal efficiency was highest when the Al/Al combination was used for all the samples. These findings indicate the possibility of

electrogenerated $Al(OH)_3$ being involved in the removal process. In other words, such a phenomenon can be explained by the fact that Al has a more significant positive standard electrode oxidation potential (E_o = +1.66 volt) in the electrochemical series than Fe (E_o = +0.44 volt) [24]. As a result, Al oxidizes more rapidly than Fe. Consequently, the oxidation of Al occurs at a faster rate than that of Fe. This leads to a higher overall production of anions during EC with an Al anode compared to a Fe anode. Consequently, the quantity of metal hydroxide flocs generated is greater with an Al anode than with a Fe anode [24]. All further investigations were conducted using a combination of Al/Al electrodes.

4.2 Effect of electrode arrangement:

Fig. 3 presents the variation in fluoride removal efficiencies for all the samples at various electrode connection modes. From all the samples, it is noticeable that removal efficiencies were highest at bipolar connection. For sample S1, the removal efficiency was found to be 87.98%, 88.35%, and 89.56%, with a corresponding residual fluoride concentration of 0.625 mg L^{-1}, 0.606 mg L^{-1}, and 0.542 mg L^{-1} for the connection mode of monopolar, series monopolar and bipolar respectively after3600 s of EC. Similar results were found for samples S2, S3, S4, and S5. The removal efficiency for monopolar, series monopolar and bipolar for S2 are 89.49%, 90.58%, 91.83%; for S3 are 93.73%, 95.29%, 96.41%; for S4, 88.84%, 90.46%, 92.61%; for S5, are 83.39%,84.24%, 87.54% respectively. The corresponding residual fluoride concentration for S2, S3, S4 and S5 are 0.395, 0.354, 0.307 mg L^{-1}; 0.564, 0.423,0.323 mg L^{-1}; 1.44, 1.23, 0.953 mg L^{-1} and 0.923, 0.876, 0.693 mg L^{-1} respectively after 3600 s of EC. The residual fluoride concentration for all the samples were found to be within permissible limit. Improved ion removal efficiency for series monopolar and bipolar mode was due to the addition of two electrodes between the anode and cathode, which induces electric charges and eventually increases the flocs

[40]. Bipolar mode resulted in higher ion removal than serial monopolar mode because the anodes undergo higher electro-dissolution than in bipolar mode [24]. Considering the higher fluoride concentration in some groundwater samples, the bipolar mode was used for conducting further experiments, to achieve adequate removal of fluoride ions.

4.3 Effect of electrical potential:

Fig. 4 shows the removal efficiencies of fluoride ions for all the samples at various electric potentials applied during the process. It can be seen from Fig. 4 that the removal efficiency of fluoride ions increases with the increase in applied electrical potential. The removal efficiency of sample S1 at the electrical potential of 6V, 9V, and 12V were 75.77%, 88.86%, and 89.58%, with a corresponding residual fluoride concentration of 1.26 mg/L, 0.579 mg/L, and 0.542 mg/L, respectively, after3600 s of EC. Similar trends are found for the other samples. The removal efficiencies with corresponding residual fluoride concentration for sample S2 are 82.74%, 89.47%, 91.84% (0.649 mg L^{-1}, 0.396 mg L^{-1}, 0.307 mg L^{-1}); for S3 are 95.71%, 96.04%, 96.41% (0.386 mg L^{-1}, 0.356 mg L^{-1}, 0.323 mg L^{-1}); for S4 are 91.86%, 92.33%, 92.61% (1.05 mg L^{-1}, 0.989 mg L^{-1}, 0.953 mg L^{-1}); for S5 are 83.94%,86.24%,87.54% (0.893 mg L^{-1}, 0.765 mg L^{-1}, 0.693 mg L^{-1}) at applied electrical potential of 6V, 9V and 12V respectively after 3600 s of EC. An increase in fluoride ion removal at higher electrode potentials was due to a higher flocs generation rate [25]. According to the fluoride ion removal mechanism during EC, the removal occurred due to adsorption of the fluoride ions by the aluminum hydroxide flocs generated, followed by coagulation and co-precipitation [25]. From the experimental results, the removal of fluoride can be explained by two mechanisms simultaneously, one due to adsorption and co-precipitation and the other due to flocculation of the pollutant ions in the solution [13]. For this study, the applied current densities at the various electric potentials of 6V, 9V, and 12V are

calculated to be 17.24 A m^{-2}, 43.10 A $m^{-2,}$ and 68.96 A $m^{-2,}$ respectively. It should be emphasized that in EC, CD controls the rate of coagulant formation, the emergence and expansion of bubbles, and the size of flocs. These factors collectively contribute significantly to the efficiency of fluoride ion removal through EC. In instances of continuous processes or groundwater with varying fluoride ion concentrations along with co-existing ions like hardness, TDS, etc., it becomes imperative to make tailored adjustments in CD. This ensures effective water treatment, maintaining fluoride ion concentration and other water quality parameters within permissible limits. Overall, at the electrical potential of 6V and 9V, residual concentration for samples S3 and S4 was higher compared to samples S1, S2, and S5, signifying that applied electrode potential below 9V was not adequate for higher fluoride ion concentration. For S3 S4, the permissible fluoride concentration level of 1.0 mg L^{-1} can be obtained for electrode potential of 12 volts and above, observed within 3600 s. These observations inferred that higher electrode potential or extended duration of EC is required to treat groundwater with high fluoride ion concentrations. Considering all these facts, the applied electrical potential of 12 V was considered for all the subsequent experiments.

Kinetic analysis was carried out using 1st order and 2nd order reaction models available in the literature [23]. However, better fitting was observed for 1st order model described in Eq 2. Table S2 shows the rate constant and R^2 values for first order kinetic plot of ln (C_o/C) vs time in a linear trend for different CD calculated as per Eqn.1 for applied potential of 6-12 V for sample S1 to S5. The values of k calculated are 0.024, 0.036 and 0.039 min^{-1} for different CD of 17.24 A m^{-2}, 43.10 A $m^{-2,}$ and 68.96 A m^{-2} respectively for sample S1. From Table S2, it can be observed that the rate of fluoride ion removal (k) increases with increasing the CD. Such an increase in k was due to the availability of higher amounts of Al^{3+} ions in the solution as described earlier.

4.4 Effect of inter-electrode distance:

Fig. 5 shows the variation in the removal efficiency of fluoride for all the samples after 3600 s of EC at various electrode distances. Fig. 5 shows that for sample S1, the removal efficiency of fluoride decreases from 89.57% to 83.38%, with an increase in ID from 0.5 cm to 2.0 cm. The corresponding residual fluoride concentration at the ID of 0.5, 1.0, 1.5, and 2.0 cm are 0.542 mg L^{-1}, 0.645 mg L^{-1}, 0.754 mg L^{-1}, and 0.864 mg L^{-1}, respectively. The removal efficiency at the ID of 0.5, 1.0, 1.5, and 2.0 cm for sample S2 are 91.83%, 91.46%, 91.12%, and 90.82% with corresponding residual fluoride concentrations of 0.307 mg L^{-1}, 0.321 mg L^{-1}, 0.334 mg L^{-1} and 0.345 mg L^{-1} respectively. Similar trends are found in samples S3, S4, and S5. The decrease in removal efficiency of fluoride or increase in residual ion concentration was due to the rise in both the resistance and the growth of the passive anodic film with higher ID, which likewise decreases the current and the amount of floc formed, affecting the removal efficiency [25]. Overall, residual concentration for samples S3 and S4 was higher than samples S1, S2 and S5 due to the presence of higher fluoride ions in samples S3 and S4. For all the samples, the permissible level of fluoride concentration i.e. 1.0 mg L^{-1} was obtained for all the IDs (0.5 – 2.0 cm) within 3600 s. Considering the above observations, a lower ID of 0.5 cm was used for all the further experiments since a larger ID involves high currents to sustain the requisite electrode potential, and pollutant ion removal effectiveness decreases [25].

4.5 Assessment of residual Fe and Al ion concentrations after EC:

Following EC treatment, the concentrations of Fe and Al ions were evaluated to determine the presence of any residual coagulant metals in the treated water. From Table 2, it was observed that across all five samples (S1 to S5), Fe levels remained below the detection limit (BDL), indicating that the EC process effectively removed the Fe ions. In contrast, Al concentrations displayed noticeable variability and, in several cases, exceeded the permissible limit of 0.2 mg/L. The highest

concentrations were observed in S1 (0.65 mg/L) and S3 (0.72 mg/L), while S2, S4, and S5 showed relatively lower values ranging from 0.17 to 0.29 mg/L. Only sample S2 met the acceptable safety threshold. These results imply that the use of aluminum-based electrodes during the EC process led to the generation of excess $Al(OH)_3$ flocs at higher applied potential, which subsequently contributed to the release of residual Al^{3+} ions into the treated water. This indicates that aluminium, while acting as a coagulant, also poses a risk of secondary pollution if not effectively removed during post-treatment stages. The elevated levels of Al in multiple samples highlight the need for effective post-treatment strategies after EC such as adsorption and optimized filtration, to ensure compliance with drinking water standards.

4.6 Effect of adsorbent dose on the removal of predominant ions:

To explore the impact of adsorption on fluoride removal after EC, analytical grade activated charcoal at various doses was considered. To estimate the equilibrium time of the adsorption process, the activated carbon of dose 1g $3L^{-1}$ was considered for all the samples post-EC treatment at a constant temperature of 25 °C for all samples. It was found that equilibrium was attained at1800 s for all the samples. This indicates that fluoride ion and activated carbon strongly interacted and shows the effectiveness of the process. To evaluate the impact of adsorbent dose on fluoride removal efficiency, adsorbent dose of 1g $3L^{-1}$, 3g $3L^{-1}$, and 5 g $3L^{-1}$ was considered at a constant temperature of 25 °C, stirring at 200 rpm for1800 s. Fig. 6 shows the changes in residual fluoride concentration for all samples at various adsorbent doses. It is observed that increasing the adsorbent dose above 1g $3L^{-1}$ dose slightly increases the removal of fluoride ion as the number of active sites available for adsorption increases for fluoride adsorption in the sample. However, increasing the dose over 3g $3L^{-1}$ seems to have little impact on fluoride removal since the cumulative solute adsorption in the unit weight of an adsorbent may decrease with increased

adsorbent dosage. It happens due to the interaction of active sites of an adsorbent [41]. However, to treat samples with higher residual fluoride in the solution after EC, the adsorbent dose may be increased for desirable removal. Table 2 and Table S3 present the water quality parameters in terms of TDS, turbidity, salinity, pH, alkalinity, hardness, sulfate, phosphate, etc., along with fluoride and Al concentration after 3600 s of EC and after 1800 s of adsorption with various adsorbent dosage respectively for sample S1 to S5. From Table S3, it is observed that the final estimated value of Al ion decreases significantly from 0.15 mg L^{-1} to 0.09 mg L^{-1} with the increase in adsorbent dose from 1g $3L^{-1}$ to 5g $3L^{-1}$ for sample S1. Similarly, for sample S1, at an adsorbent dose of 1g $3L^{-1}$, 3 g $3L^{-1}$, and 5 g $3L^{-1}$ the final values of TDS are: 452, 423, and 418 mg L^{-1}, turbidity are: 0.1, 0.08, and 0.07 NTU, conductivity are: 541, 524 and 502 µs/cm, alkalinity is: 195, 155 and 145 mg L^{-1}, hardness are: 80, 75 and 70 mg L^{-1}, pH are: 7.02, 7.01 and 7.01, sulfate are: 175, 152 and 150 mg L^{-1}, nitrate is: 2.2, 1.8, 1.6 mg L^{-1}, phosphate are: 0.08, 0.06 and 0.05 mg L^{-1}, chorine are: 0.25, 0.18 and 0.21 mg L^{-1}, calcium are: 58, 50, and 50 mg L^{-1} Mg are: 22, 25 and 21 mg L^{-1} and potassium are: 2.7, 1.7 and 1.5 mg L^{-1} respectively after1800 s of adsorption. Similar results are found for all the other samples. However, the removal efficiency of all the parameters improved after adsorption at various doses compared to only EC treatment (Table 2) for all the samples. But for all the subsequent experiments, a lower adsorbent dose of 1g $3L^{-1}$ was considered as all the final values for all the dosages were within permissible limits.

4.7 Comparison of various filtration mediums:

To compare the effectiveness of various filtration mediums for separating the flocs generated during EC and adsorption, filter paper, a commercially available ceramic candle-based filter, and a gravity carbon filter were considered. The variation in fluoride ion concentration at various filtration medium for all the samples are presented in Fig. 7. It is observed from Fig. 7 that the

387 removal of fluoride is slightly improved using a ceramic filter compared to filter paper and gravity
388 carbon filter for all the samples. For sample S1, the residual fluoride concentration using filter
389 paper, ceramic filter, and gravity carbon filter is 0.334 mg L^{-1}, 0.278 mg L^{-1}, and 0.33 mg L^{-1},
390 respectively. Similar results were also found for all the samples. Such slight improvement in
391 fluoride ion removal using a ceramic filter may be due to the degradation of the pollutant ion or
392 adsorptive reduction during the separation process [42]. The water quality parameters of all the
393 sample's supernatant using various filtration modes are presented in Table S4. For sample S1, the
394 final values of fluoride, Al, sulfate, nitrate, phosphate ion, and alkalinity are slightly less in the
395 case of ceramic filtration compared to filter paper due to its adsorptive removal ability. Natural
396 clay present in the ceramic filter membrane serves as an effective absorbent in the process of
397 eliminating contaminants and pollutants from water [43]. But the final values of TDS were found
398 to increase from 452 mg L^{-1} to 455 mg L^{-1}, turbidity from 0.1 to 0.15 NTU, chlorine from 0.25 to
399 0.48 mg L^{-1}, hardness from 80 to 101 mg L^{-1} and calcium ion from 18 to 54 in case of filter paper
400 and ceramic filtration respectively for sample S1. Such an increase in final residual concentrations
401 in the supernatant of ceramic filtration may be due to the precursors used during the manufacture
402 of such ceramic-candle filters, which dissolve during the separation process and may be retained
403 in the supernatant. The concentration of Fe ions across all samples (S1 to S5) for all filtration
404 media was below the detection limit, indicating that iron was present at extremely low levels,
405 undetectable by standard analytical methods. In contrast, the concentration of Al varied
406 significantly depending on the type of filtration medium used. Samples filtered through filter paper
407 exhibited the highest aluminium concentrations, ranging from 0.12 to 0.52 mg/L, with several
408 values exceeding the permissible limit. The ceramic filter demonstrated improved performance,
409 reducing aluminium concentrations to a range of 0.11 to 0.19 mg/L, all within the permissible

limit. Notably, the gravity carbon filter showed the highest efficiency, consistently maintaining aluminium concentrations between 0.10 and 0.15 mg/L across all samples.

However, all the values were found within permissible limits, and no compromise in the treated water's color and odor was found. Moreover, gravity carbon filtration has also shown desirable results for all the parameters. A ceramic candle filtration unit is known to be a cost-effective technology for the purification of drinking water due to its compact footprint, simple operation and cost-effective [42]. Nevertheless, when it comes to ceramic candle filters, a gradual reduction in flow rate over time may occur, attributed to clogging by suspended particles. This potential issue can be addressed by implementing mild scrubbing procedures after a specific period of usage [44]. Inspired by this, a novel integrated process of EC combined with adsorption and subsequent ceramic candle-based filtration treatment unit can be developed for effective household drinking water purification or on a large scale for defluoridation along with removal of secondary pollutants.

4.8 Estimation of EEC, electrode consumption, theoretical H_2 gas yield, and TC:

The EEC for treating 3 L of water for3600 s was estimated to be 0.4, 1.5, and 3.2 kWh m^{-3} for electrical potential of 6, 9, and 12 V (i.e. CD of 17.24 A m^{-2}, 43.10 A/m^{-2}, and 68.96 A m^{-2}) respectively. The electrode consumption at 6, 9, and 12 V was estimated to be 0.0671, 0.1677, and 0.2684 g L^{-1}, respectively. The consumption of electrode and EEC increases with an increase in electric potential due to the faster dissolution of the electrode at higher current density. Additionally, it's worth noting that there's a risk of excess anodic corrosion at higher current density, leading to the release of excess Al^{3+} ions. This leads to the accumulation of Al^{3+} ions at the top of the EC reactor influenced by the bubble buoy effect, and in some instances, these Al^{3+} ions may enter the solution, persisting as a secondary pollutant in the water [24].

The theoretical H_2 gas production at CD of 17.24 A m^{-2}, 43.10 A $m^{-2,}$ and 68.96 A m^{-2} are 0.0895 L, 0.2237 L, and 0.3581 L respectively after3600 s of EC as per mentioned in Eq. 2. The amount of yieldable energy from this amount of H_2 gas as per Eqn.3 can be estimated as 9.028×10^{-4}, 2.27×10^{-3}, 3.64×10^{-3} MJ which is equivalent to 6.27, 15.76, 25.28 kW m^{-3} for CD of 17.24 A m^{-2}, 43.10 A $m^{-2,}$ and 68.96 A m^{-2} respectively. The estimated values infer that the amount of H_2 production increases as the CD increases. The production of H_2 leads to the formation of a substantial quantity of liquid foam on the reactor solution's surface. This foam aids in pollutant removal through air flotation. EC plants hold the potential to generate a significant amount of energy, which can, in turn, be utilized for the operation of these plants.

The operational expenses of the EC process after 3600 s of reaction at various electrical potentials, i.e., 6, 9, and 12 V, are calculated to be 0.0883, 0.2676, and 0.5030 US$ $m^{-3,}$ respectively. The operating cost increased at higher electric potential due to higher electrode and energy consumption. However, depending upon the quality of groundwater and the contaminant's concentration, the operating parameters of EC, mainly CD, can be altered, which may lead to inevitable fluctuation in operating cost, EEC, electrode consumption, and theoretical H_2 generation. The total estimated operational cost for the integrated process combining EC, adsorption and filtration was found to be 0.1038 US$ m^{-3}, 0.2831 US$ m^{-3} and 0.5185 US$ m^{-3} calculated as per Eqn. 8. for EC operated at electric potential of 6, 9 and 12V respectively and activated carbon dosage of 3g $3L^{-1}$.

4.9 Characterization of the sludge generated from the EC bath:

Fig. S1 shows the FESEM and EDX analysis of the electrochemical sludge for S1 to S5. The morphology and texture of the sludge show spherical-like agglomerated particles formed through the precipitation mechanism. The texture of the sludge is seen to have varying pore sizes on the s

EDX analysis in terms of atomic % is presented in Table S5 for all samples. It confirms the sludge's presence of fluoride, Al, Na, Mg, Fe, Si, Cl, and other trace elements. The weight percentage for fluoride for all the samples is between 0.55 and 1.27, and Al is 26.17 to 35.23, confirming that the amount of $Al(OH)_3$ flocs required for efficient fluoride removal is extremely high. This is due to the other co-existing contaminants in all the samples in higher concentrations, which are removed simultaneously during the process. Because contaminants and metal hydroxide particles, which are redox-active materials, are physically removed during the water treatment process and deposited in another substrate (sludge), reusing them as electrocatalysts might be an effective toxic waste management technique [45].

4.10 Design of a batch EC-based hybrid treatment unit:

Based on the experimental data presented in the previous section, it can be observed that electric potential and operating time are the most important parameters that can be altered as per requirement. Considering the kinetic results presented in section 4.3, a calculation has been conducted to identify the desirable electric potential required for treating different fluoride-contaminated water concentrations. Fig S2 shows the schematic diagram of the batch EC-based treatment unit on the results obtained from the present work integrating adsorption and ceramic membrane filtration. Based on the data shown in Table S2, the first-order rate constant varied with electric potential for the sample S4 can be rewritten as follows:

$$k = 0.0007\,V + 0037 \tag{10}$$

Using this value of k, Eq. 2 may be modified as

$$C_f = C_0 \,.\, e^{-(0.0007V + 0.037).t} \tag{11}$$

476 Where C_o, C_f , V and t are the initial fluoride concentration (mg/L), final fluoride concentration
477 (mg/L), electric potential (Volt) and time of EC (sec) respectively. Fig. 8 shows the predicted
478 residual fluoride concentration after 3600 s of EC at different electric potential for various initial
479 fluoride concentration (5, 7, 9, 11, 13, 15, 20, 25, 30 mg L^{-1}). The design is outlined for a batch
480 EC treatment unit. For example to treat initial concentration of 5-9 mg L^{-1}, electric potential of 1
481 volt and 3600 s treatment time is sufficient to achieve residual concentration below 1mg L^{-1}.
482 Similarly for higher initial concentration of above 11 up to 30 mg L^{-1}, higher potential of 12 volts
483 will be suitable. It is also to be noted that for treating higher concentration samples, lower potential
484 will also be favourable if we increase the time of treatment and vice-versa.

485 **5. Conclusion**

486 This study assessed the effectiveness of EC using aluminum electrodes in bipolar configuration
487 for treating fluoride-contaminated groundwater. Under optimized EC conditions of 12 V potential,
488 0.5 cm electrode gap, and 3600 s of treatment, fluoride concentrations in five groundwater samples
489 were reduced to below the WHO's recommended limit, with removal efficiencies ranging from
490 93.45% to 99.82%. However, certain water quality parameters, including TDS, alkalinity,
491 magnesium, and aluminium ions, remained above acceptable limits following electrocoagulation
492 alone. A subsequent adsorption step using activated charcoal (1 g per 3 L for 1800 s) further
493 improved fluoride removal and significantly reduced residual contaminants. For sample S1, final
494 concentrations of TDS, alkalinity, magnesium and total Al were further reduced to 452 mg L^{-1},
495 195 mg L^{-1}, 62 mg L^{-1} 0.15 mg L^{-1} respectively, along with the improved removal for all other
496 coexisting ions with similar trends observed for other samples. Additional treatment through
497 ceramic and carbon filtration further enhanced water quality, bringing all parameters within
498 permissible limits. Theoretical hydrogen gas yield increased with current density, reaching 0.3581

L at 68.96 A m^{-2} after 3600 s of EC. Sludge characterization by FESEM and EDX analysis confirmed the capture of fluoride and associated ions by metal hydroxide flocs. Kinetic analysis indicated that fluoride removal followed a first-order model. At an applied potential of 12 V, energy consumption, electrode consumption, and operating cost were estimated at 3.2 kWh m^{-3}, 0.2684 g L^{-1}, and 0.5030 US$ m^{-3}, respectively. The integrated treatment process, including adsorption and filtration, marginally increased the total operational cost to 0.5185 US$ m^{-3}. These findings demonstrate the technical feasibility of a combined electrocoagulation–adsorption–filtration approach for developing an EC-based household drinking water purification unit targeting groundwater pollutants. However, further field-scale evaluations and long-term studies are necessary to assess the robustness and scalability of this approach for decentralized water treatment applications.

Funding Declarations: No funding was received for conducting this study

References:

[1] Alarcón-Herrera, M. T., Martin-Alarcon, D. A., Gutiérrez, M., Reynoso-Cuevas, L., Martín-Domínguez, A., Olmos-Márquez, M. A., Bundschuh, J. (2020). Co-occurrence, possible origin, and health-risk assessment of arsenic and fluoride in drinking water sources in Mexico: Geographical data visualization. *Science of the Total Environment, 698*, 134168. https://doi.org/10.1016/j.scitotenv.2019.134168

[2] Barathi, M., Kumar, A. S. K., Rajesh, N. (2019). Impact of fluoride in potable water–An outlook on the existing defluoridation strategies and the road ahead. *Coordination Chemistry Reviews, 387*, 121-128. https://doi.org/10.1016/j.ccr.2019.02.006

[3] Sadhu, M., Bhattacharya, P., Vithanage, M., Sudhakar, P. P. (2021). Adsorptive removal of fluoride using biochar–a potential application in drinking water treatment. *Separation and Purification Technology, 278*, 119106. https://doi.org/10.1016/j.seppur.2021.119106

[4] Karunanidhi, D., Aravinthasamy, P., Subramani, T. et al. Risk of Fluoride-Rich Groundwater on Human Health: Remediation Through Managed Aquifer Recharge in a Hard Rock Terrain, South India. *Natural Resources Research, 29*, 2369–2395 (2020). https://doi.org/10.1007/s11053-019-09592-4.

[5] Thapa, R., Gupta, S., Kaur, H., Baski, R. (2019). Assessment of groundwater quality scenario in respect of fluoride and nitrate contamination in and around Gharbar village, Jharkhand, India. *HydroResearch, 2,* 60-68. https://doi.org/10.1016/j.hydres.2019.09.002

[6] Chandrajith, R., Diyabalanage, S., Dissanayake, C. B. (2020). Geogenic fluoride and arsenic in groundwater of Sri Lanka and its implications to community health. *Groundwater for sustainable development, 10*, 100359. https://doi.org/10.1016/j.gsd.2020.100359

[7] Tirkey, P., Bhattacharya, T., Chakraborty, S. (2018). Optimization of fluoride removal from aqueous solution using Jamun (Syzygium cumini) leaf ash. *Process Safety and Environmental Protection, 115,* 125-138. https://doi.org/10.1016/j.psep.2017.10.022

[8] Patolia, P., Sinha, A. (2017). Fluoride contamination in Gharbar Village of Dhanbad District, Jharkhand, India: source identification and management. *Arabian Journal of Geosciences 10, (17)* 1-10. https://doi.org/10.1007/s12517-017-3164-0

[9] Van Dyke, N., Yenugadhati, N., Birkett, N. J., Lindsay, J., Turner. M. C., Willhite, C. C., Krewski, D. (2021). Association between aluminum in drinking water and incident Alzheimer's disease in the Canadian Study of Health and Aging cohort. *Neurotoxicology,83*, 157-165. https://doi.org/10.1016/j.neuro.2020.04.002

[10] Gaskin, J., Gomes, J., Darshan, S., Krewski, D. (2017). Burden of neurological conditions in Canada. *Neurotoxicology, 61*, 2-10. https://doi.org/10.1016/j.neuro.2016.05.001

[11] Liyanage, D. N. D., Diyabalanage, S., Dunuweera, S. P., Rajapakse, S., Rajapakse, R. M. G., Chandrajith, R. (2022). Significance of Mg-hardness and fluoride in drinking water on chronic kidney disease of unknown etiology in Monaragala, Sri Lanka. *Environmental Research, 203*, 111779. https://doi.org/10.1016/j.envres.2021.111779

[12] Graça, N. S., Ribeiro, A. M., Rodrigues, A. E. (2019). Modeling the electrocoagulation process for the treatment of contaminated water. *Chemical Engineering Science, 197,* 379-385. https://doi.org/10.1016/j.ces.2018.12.038.

[13] Damtie, M. M., Woo, Y. C., Kim, B., Hailemariam, R. H., Park, K. D., Shon, H. K., Park, C., Choi, J. S. (2019). Removal of fluoride in membrane-based water and wastewater treatment technologies: Performance review. *Journal of Environmental Management, 251*, 109524. https://doi.org/10.1016/j.jenvman.2019.109524.

[14] Gong, W. X., Qu, J. H., Liu, R. P., Lan, H. C. (2012). Effect of aluminum fluoride complexation on fluoride removal by coagulation. *Colloids and Surfaces A: Physicochemical and Engineering Aspects, 395,* 88-93. https://doi.org/10.1016/j.colsurfa.2011.12.010

[15] Grzegorzek, M., Majewska-Nowak, K., Ahmed, A. E. (2020). Removal of fluoride from multicomponent water solutions with the use of monovalent selective ion-exchange membranes. *Science of the Total Environment, 722,* 137681.https://doi.org/10.1016/j.scitotenv.2020.137681

[16] Wendimu, G., Zewge, F., Mulugeta, E. (2017). Aluminium-iron-amended activated bamboo charcoal (AIAABC) for fluoride removal from aqueous solutions. *Journal of Water Process Engineering, 16,* 123-131. https://doi.org/10.1016/j.jwpe.2016.12.012

[17] Nabbou, N., Belhachemi, M., Boumelik, M., Merzougui, T., Lahcene, D., Harek, Y., Zorpas, A. A., Jeguirim, M. (2019). Removal of fluoride from groundwater using natural clay (kaolinite): Optimization of adsorption conditions. *Comptes Rendus Chimie, 22(2-3),* 105-112. https://doi.org/10.1016/j.crci.2018.09.010

[18] Singh, S., German, M., Chaudhari, S., Sengupta, A. K. (2020). Fluoride removal from groundwater using zirconium impregnated anion exchange resin. *Journal of Environmental Management, 263*, 110415. https://doi.org/10.1016/j.jenvman.2020.110415

[19] Aoudj, S., Khelifa, A., Drouiche, N., Belkada, R., Miroud, D. (2015). Simultaneous removal of chromium (VI) and fluoride by electrocoagulation–electroflotation: application of a hybrid Fe-Al anode. *Chemical Engineering Journal, 267*, 153-162. https://doi.org/10.1016/j.cej.2014.12.081.

[20] Hashim, K. S., Shaw, A., Al Khaddar, R., Pedrola, M. O., Phipps, D. (2017). Iron removal, energy consumption and operating cost of electrocoagulation of drinking water using a new flow column reactor. *Journal of Environmental Management, 189,* 98-108. https://doi.org/10.1016/j.jenvman.2016.12.035

[21] Asaithambi. P., Govindarajan, R. (2021). Hybrid Sono-Electrocoagulation Process for the Treatment of Landfill Leachate Wastewater: Optimization through a Central Composite Design Approach. *Environmental Process, 8,* 793–816. https://doi.org/10.1007/s40710-021-00509-z.

[22] Nayebi, B., Ghalebizade, M., Niavol, K.P. (2021). Removal of Acid Red 131 by Peroxi-Coagulation Using Stainless Steel and Aluminum Electrodes: a Comparative Study. *Water Conservation Science Engineering* 6, 201–211. https://doi.org/10.1007/s41101-021-00114-z.

[23] Das, D., Nandi, B. K. (2022). Removal of co-existing Fe (II), As (V), and fluoride ions from groundwater by electrocoagulation. *Groundwater for Sustainable Development, 17*, 100752. https://doi.org/10.1016/j.gsd.2022.100752

[24] Das, D., Nandi, B.K. (2023). Simultaneous Removal of Coexisting Fe(II) and Cr(VI) from Wastewater by Electrocoagulation (EC) Process Using Different Types of Connection Modes. *Water Conservation Science and Engineering* 8, 25.https://doi.org/10.1007/s41101-023-00200-4

[25] Das, D., Nandi, B. K. (2021). Treatment of iron ore beneficiation plant process water by electrocoagulation. *Arabian Journal of Chemistry, 14(1)*, 102902. https://doi.org/10.1016/j.arabjc.2020.11.008.

[26] Mohtashami, R., Shang, J. Q. (2019). Electroflotation for Treatment of Industrial Wastewaters: A Focused Review. *Environmental Processes, 6,* 325–353. https://doi.org/10.1007/s40710-019-00348-z.

[27] Sahu, S., Yadav, M. K., Gupta, A. K., Uddameri, V., Toppo, A. N., Maheedhar, B., Ghosal, P. S. (2022). Modeling defluoridation of real-life groundwater by a green adsorbent aluminum/olivine composite: Isotherm, kinetics, thermodynamics and novel framework based on artificial neural network and support vector machine. *Journal of Environmental Management, 302*, 113965. https://doi.org/10.1016/j.jenvman.2021.113965.

[28] Sattar, M. S., Shakoor, M. B., Ali, S., Rizwan, M., Niazi, N. K., & Jilani, A. (2019). Comparative efficiency of peanut shell and peanut shell biochar for removal of arsenic from water. *Environmental science and pollution research*, *26*, 18624-18635.

https://doi.org/10.1007/s11356-019-05185-z

[29] Patel, M. G., Marakana, P. G., Dey, A., Saini, B., & Chokshi, H. (2023). Coal fly ash derived adsorbent for enhancing waste water treatment. *Materials Today: Proceedings*, *77*, 163-167.https://doi.org/10.1016/j.matpr.2022.11.111

[30] Ahmaruzzaman, M., & Gupta, V. K. (2011). Rice husk and its ash as low-cost adsorbents in water and wastewater treatment. *Industrial & Engineering Chemistry Research*, *50*(24), 13589-13613. https://doi.org/10.1021/ie201477

[31] Chingono, K. E., Sanganyado, E., Bere, E., & Yalala, B. (2018). Adsorption of sugarcane vinasse effluent on bagasse fly ash: A parametric and kinetic study. *Journal of environmental management*, *224*, 182-190.https://doi.org/10.1016/j.jenvman.2018.07.042

[32] De, S., Hazra, T., Dutta, A. (2022). Application of integrated sequence of air stripping, coagulation-flocculation, electrocoagulation and adsorption for sustainable treatment of municipal landfill leachate. *Cleaner Waste Systems, 3*, 100033. https://doi.org/10.1016/j.clwas.2022.100033.

[33] Kar, S., Gupta, R. (2023). Fluoride Toxicity in Rajasthan, India: Human Health Risk Assessment, Low-Cost Water Filter Preparation, and Contaminant Remediation. *Water Conservation Science and Engineering* 8, 3. https://doi.org/10.1007/s41101-023-00175-2

[34] Kumari, N., Pathak, G. (2014). A review of groundwater quality issue in Jharkhand due to fluoride. *International Journal of Engineering Research and Applications, 4(3),* 65-77.

[35] Bhat, S., Uthappa, U. T., Sadhasivam, T., Altalhi, T., Han, S. S., Kurkuri, M. D. (2023). Abundant cilantro derived high surface area activated carbon (AC) for superior adsorption performances of cationic/anionic dyes and supercapacitor application. *Chemical Engineering Journal*, *459*, 141577. https://doi.org/10.1016/j.cej.2023.141577

[36] Oladipo, A. A., Mustafa, F. S., Ezugwu, O. N., Gazi, M.(2022). Efficient removal of antibiotic in single and binary mixture of nickel by electrocoagulation process: Hydrogen generation and cost analysis. *Chemosphere, 300*, 134532. https://doi.org/10.1016/j.chemosphere.2022.134532

[37] Phalakornkule, C., Sukkasem, P., Mutchimsattha, C. (2010). Hydrogen recovery from the electrocoagulation treatment of dye-containing wastewater. *International Journal of Hydrogen Energy, 35,* 10934-10943. https://doi.org/10.1016/j.ijhydene.2010.06.100.

[38] Dhadge, V. L., Medhi, C. R., Changmai, M., Purkait, M. K. (2018). Household unit for the treatment of fluoride, iron, arsenic and microorganism contaminated drinking water. *Chemosphere, 199,* 728-736. https://doi.org/10.1016/j.chemosphere.2018.02.087

[39] Chaudhuri, Malay, Sanjeev R. Verma, and Anirban Gupta. "Performance evaluation of ceramic filter candles." *Journal of Environmental Engineering* 120, no. 6 (1994): 1646-1651. https://doi.org/10.1061/(ASCE)0733-9372(1994)120:6(1646).

[40] Xu, R., Yang, Z., Niu, Y., Xu, D., Wang, J., Han, J., Wang, H. (2022). Removal of microplastics and attached heavy metals from secondary effluent of wastewater treatment plant using interpenetrating bipolar plate electrocoagulation. *Separation and Purification Technology, 290,* 120905. https://doi.org/10.1016/j.seppur.2022.120905

[41] Senewirathna, D. S. G. D., Thuraisingam, S., Prabagar, S., Prabagar, J. (2022). Fluoride removal in drinking water using activated carbon prepared from palmyrah (Borassus flabellifer) nut shells. *Current Research in Green and Sustainable Chemistry, 5,*100304. https://doi.org/10.1016/j.crgsc.2022.100304

[42] Mustapha, S., Oladejo, T. J., Muhammed, N. M., Saka, A. A., Oluwabunmi, A. A., Abdulkabir, M., Joel, O. O. (2021). Fabrication of porous ceramic pot filters for adsorptive removal of pollutants in tannery wastewater. *Scientific African, 11,* e00705. https://doi.org/10.1016/j.sciaf.2021.e00705

[43] Wang, S., Wu. Q., Yan, B., Guo, Y., Xia, W., Li, J., Cui, F., Tian, J. (2022). A novel integrated process of ceramic membrane filtration coupled with peroxymonosulfate activation and adsorption for water treatment. *Separation and Purification Technology, 291*,120874. https://doi.org/10.1016/j.seppur.2022.120874

[44] Cai, C., Sun, W., He, S. Zhang Y., Wang X. (2023). Ceramic membrane fouling mechanisms and control for water treatment. *Front. Environ. Sci. Eng.* 17, 126. https://doi.org/10.1007/s11783-023-1726-9

[45] Babu, D. S., Vijay, K., Nidheesh, P. V., Kumar, M. S. (2021). Performance of continuous aerated iron electrocoagulation process for arsenite removal from simulated groundwater and management of arsenic-iron sludge. *Sustainable Energy Technologies and Assessments, 47*, 101476. https://doi.org/10.1016/j.seta.2021.101476.

List of Tables:

Table 1: Various water quality parameters of the collected water sample.

Parameters	Sample 1	Sample 2	Sample 3	Sample 4	Sample 5	Permissible limit [1]
Fluoride (mg L^{-1})	5.2	3.76	8.99	12.9	5.56	1
Al (mg L^{-1})	4.42	1.63	3.46	0.9196	3.3653	0.2
Fe (mg L^{-1})	0.007	0.1207	0.0208	0.014	0.371	0.30-0.50
TDS (mg L^{-1})	1570	828	1610	532	1189	500-700
Turbidity (NTU)	1.07	5.6	3.86	2.3	10.31	<1
Conductivity (µS cm^{-1})	2173	1150	2228	731	1647	200-2000
Salinity (mg L^{-1})	1198	392	1240	231	834	-
pH	7.45	7.65	7.94	7.56	7.66	6.5-8.5
Sulphate (mg L^{-1})	510	81	205	12	126	250
Nitrate (mg L^{-1})	5.2	2.9	4.77	2.41	3.09	10
Phosphate (mg L^{-1})	3.2	0.43	0.44	0.24	2.5	0.1
Chlorine (mg L^{-1})	0.33	0.22	0.17	0.13	0.2	4
Alkalinity (mg L^{-1})	650	205	651	195	450	200
Hardness (mg L^{-1})	460	45	215	30	360	200
Ca^{2+} (mg L^{-1})	102	10	19	5	22	60
Mg^{2+}(mg L^{-1})	358	35	196	25	338	30
K^{-}(mg L^{-1})	4.5	2	2.9	1.3	3.7	10

672 Table 2: Water quality parameters for all samples after 3600 s of EC at optimum condition.

673 Electric potential: 12V, ID: 0.5 cm, Electrode: Al/Al, Electrode mode: Bipolar

Parameters	S1	S2	S3	S4	S5	Permissible limit [1]
Fluoride (mg L^{-1})	0.542	0.307	0.323	0.953	0.693	1
Al (mg L^{-1})	0.65	0.17	0.72	0.22	0.29	0.2
Fe (mg L^{-1})	BDL	BDL	BDL	BDL	BDL	0.30-0.50
TDS (mg L^{-1})	556	280	582	256	511	500-700
Turbidity (NTU)	0.5	1.1	0.85	0.94	2.05	<1
Conductivity (µS cm^{-1})	562	556	674	471	692	200-2000
Salinity (mg L^{-1})	242	254	355	375	282	-
pH	7.12	7.16	7.45	7.28	7.35	6.5-8.5
Sulphate (mg L^{-1})	184	29	162	6	92	250
Nitrate (mg L^{-1})	2.4	1.22	1.82	1.12	1.28	10
Phosphate (mg L^{-1})	0.11	0.07	0.05	0.06	0.08	0.1
Chlorine (mg L^{-1})	0.26	0.18	0.1	0.09	0.18	4
Alkalinity (mg L^{-1})	245	145	249	95	184	200
Hardness (mg L^{-1})	103	43	86	19	184	200
Ca^{2+} (mg L^{-1})	26	7	15	4	19	60
Mg^{2+} (mg L^{-1})	77	36	71	15	165	30
K^{-} (mg L^{-1})	2.9	1.2	1.5	0.85	1.8	10

674

675 **List of Figures:**

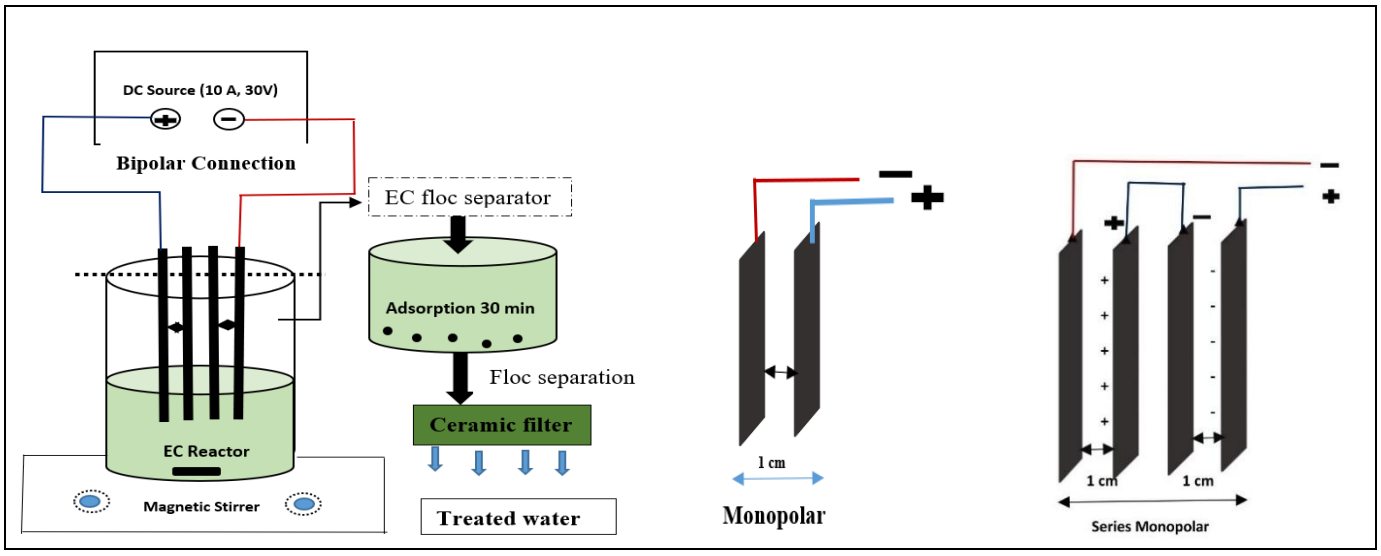

676 **Fig. 1**: Schematic diagram of the experimental setup showing various connection mode.

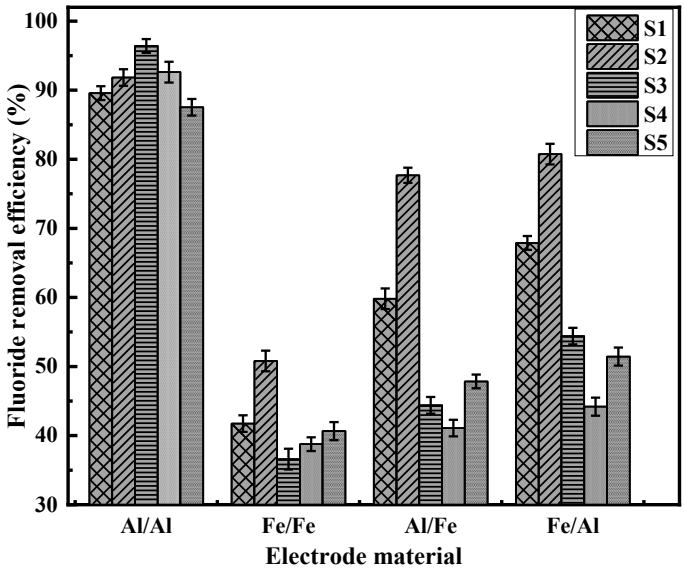

677

678 **Fig. 2:** Effect of various electrode material on fluoride removal efficiency for S1, S2, S3, S4 and
679 S5. Reaction conditions: Electric potential: 12 V, Electrode mode: Bipolar, EC time: 3600 s, ID:
680 0.5 cm.

681

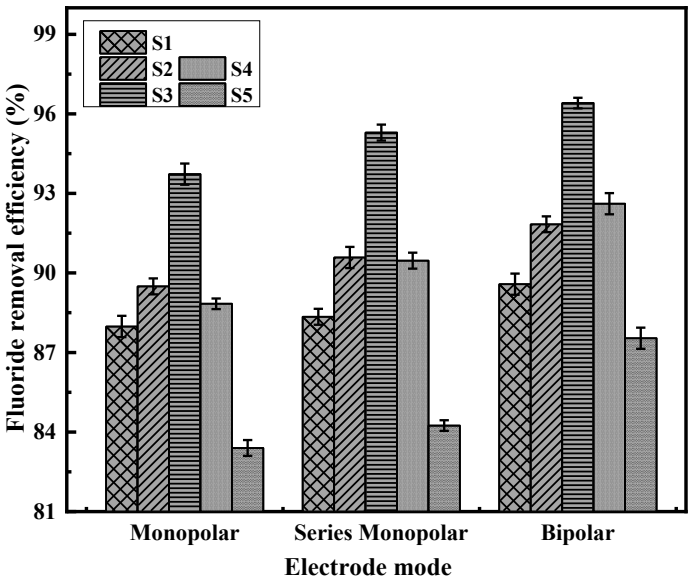

682

683 **Fig. 3:** Effect of various electrode mode on fluoride removal efficiency for S1, S2, S3, S4 and S5.
684 Reaction conditions: Electric potential: 12 V, Electrode material: Al/Al, EC time: 3600 s, ID: 0.5
685 cm.

686

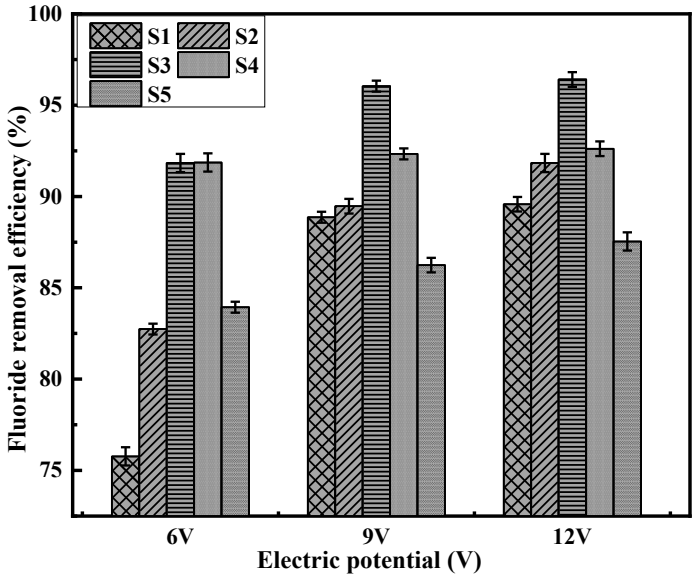

687

688 **Fig. 4:** Effect of various electrical potential on fluoride removal efficiency for S1, S2, S3, S4 and
689 S5. Reaction conditions: Electrode mode: Bipolar, Electrode material: Al/Al, EC time: 3600 s, ID:
690 0.5 cm.

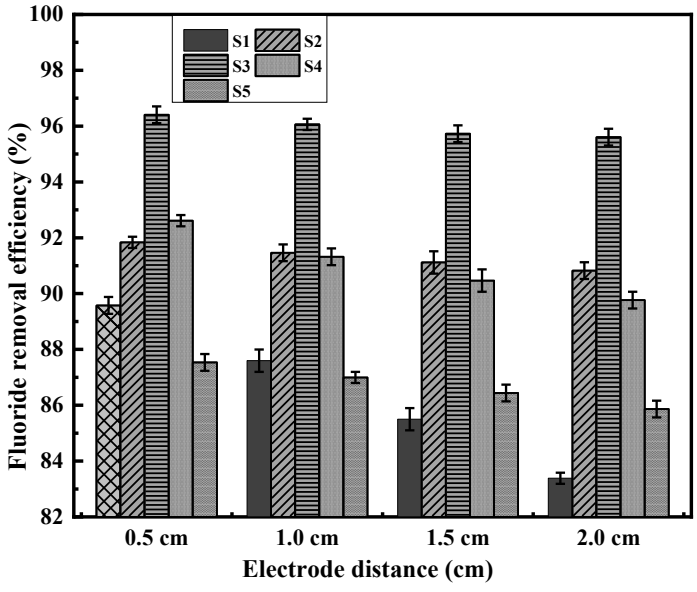

691

692 **Fig. 5:** Effect of various electrode distance on fluoride removal efficiency for S1, S2, S3, S4 and
693 S5. Reaction conditions: Electric potential: 12 V, Electrode material: Al/Al, Electrode mode:
694 Bipolar, EC time: 3600 s.

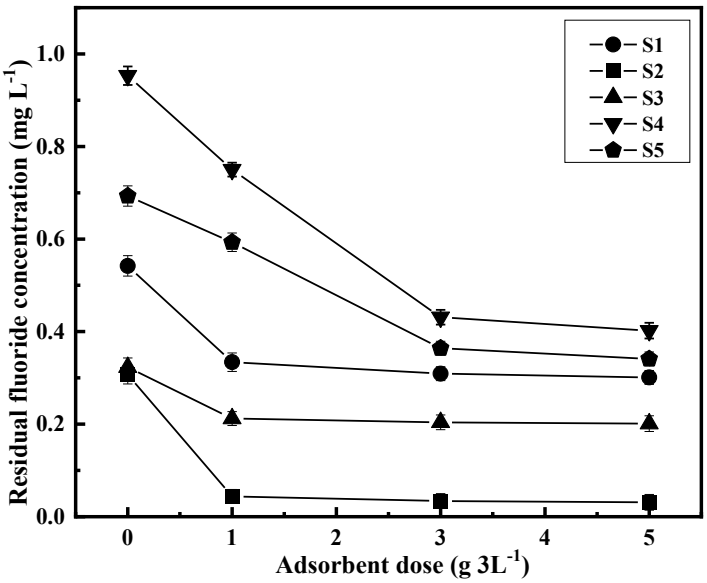

Fig. 6: Residual fluoride concentration at various adsorbent dose at adsorption time1800 s. Reaction conditions: Electric potential: 12 V, Electrode material: Al/Al, Electrode mode: Bipolar, EC time: 3600 s, ID: 0.5 cm.

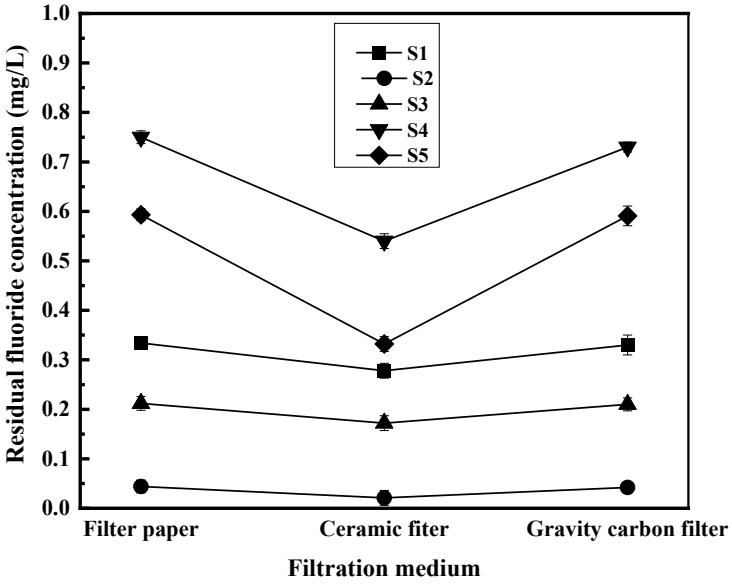

Fig. 7: Residual fluoride concentration for various filtration medium. Reaction conditions: For EC: Electric potential: 12 V, Electrode material: Al/Al, Electrode mode: Bipolar, EC time: 3600 s, ID: 0.5 cm. For adsorption: adsorbent dose: 3g $3L^{-1}$, adsorption time:1800 s.

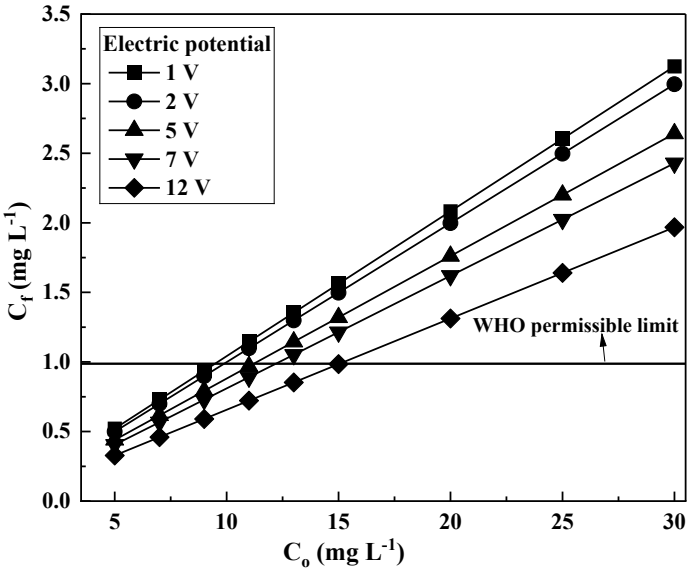

704

705 **Fig. 8**: Predicted residual fluoride concentration for different concentrations of real groundwater
706 sample contaminated with fluoride at different electric potential (V). [EC experiment conditions:
707 ID: 0.5 cm, Electrode: Al/Al, Electrode mode: Bipolar]

708